

Available online at www.sciencedirect.com

ScienceDirect

journal homepage: www.elsevier.com/locate/watres

Biomining of arsenate to arsenic sulfides is greatly enhanced at mildly acidic conditions

Lucia Rodriguez-Freire^{a,*}, Reyes Sierra-Alvarez^a, Robert Root^b,
Jon Chorover^b, James A. Field^a

^a Department of Chemical and Environmental Engineering, The University of Arizona, P.O. Box 210011, Tucson, AZ, USA

^b Department of Soil, Water and Environmental Science, The University of Arizona, P.O. Box 210038, Tucson, AZ, USA

ARTICLE INFO

Article history:

Received 6 November 2013

Received in revised form

13 August 2014

Accepted 14 August 2014

Available online 24 August 2014

Keywords:

Arsenate reduction

Sulfate reduction

Bioprecipitation

Orpiment

Realgar

Biomining

ABSTRACT

Arsenic (As) is an important water contaminant due to its high toxicity and widespread occurrence. Arsenic-sulfide minerals (ASM) are formed during microbial reduction of arsenate (As^V) and sulfate (SO₄²⁻). The objective of this research is to study the effect of the pH on the removal of As due to the formation of ASM in an iron-poor system. A series of batch experiments was used to study the reduction of SO₄²⁻ and As^V by an anaerobic biofilm mixed culture in a range of pH conditions (6.1–7.2), using ethanol as the electron donor. Total soluble concentrations and speciation of S and As were monitored. Solid phase speciation of arsenic was characterized by x-ray adsorption spectroscopy (XAS). A marked decrease of the total aqueous concentrations of As and S was observed in the inoculated treatments amended with ethanol, but not in the non-inoculated controls, indicating that the As-removal was biologically mediated. The pH dramatically affected the extent and rate of As removal, as well as the stoichiometric composition of the precipitate. The amount of As removed was 2-fold higher and the rate of the As removal was up to 17-fold greater at pH 6.1 than at pH 7.2. Stoichiometric analysis and XAS results confirmed the precipitate was composed of a mixture of orpiment and realgar, and the proportion of orpiment in the sample increased with increasing pH. The results taken as a whole suggest that ASM formation is greatly enhanced at mildly acidic pH conditions.

© 2014 Elsevier Ltd. All rights reserved.

1. Introduction

Arsenic (As) contamination of natural waters is a major health and environmental concern. The United States Environmental Protection Agency (US-EPA) have set the As standard in drinking water at 10 ppb (US-EPA, 2001). The concentration of As in groundwater and drinking water

exceeds this limit in many locations across the world (Murcott, 2012). Elevated As concentrations generally occur due to As mobilization from high As-content rocks and sediments driven by changes under the biogeochemical conditions of the aquifer (Welch et al., 2000), therefore a better understanding of the biogeochemistry of As is necessary to predict and control As mobilization and to remediate As contaminated waters.

* Corresponding author. Tel.: +1 520 621 2591; fax: +1 520 621 6048.

E-mail address: luciar@email.arizona.edu (L. Rodriguez-Freire).

<http://dx.doi.org/10.1016/j.watres.2014.08.016>

0043-1354/© 2014 Elsevier Ltd. All rights reserved.

Arsenopyrite (FeAsS), realgar (AsS) and orpiment (As₂S₃) are naturally formed As-bearing sulfide minerals (ASM) (O'Day et al., 2004) which are known to be a source of As contamination due to weathering processes that dissolve the mineral and release the retained As into the environment (Welch et al., 2000). However, the formation of ASM can be harnessed to promote the immobilization of As. The biogeochemical cycle of As is dominated by the microbial transformations between the two main inorganic species of As, arsenate (As^V, H₂AsO₄⁻ and HAsO₄²⁻ in circumneutral environments) and arsenite (As^{III}, H₃AsO₃) (van Lis et al., 2013). In oxidizing environments, As^V is the predominant species, and the accumulation of As is limited by sorption processes of As on iron (Fe) oxides and oxyhydroxides surfaces (Jonsson and Sherman, 2008); in reducing environments, As^V can be microbially reduced to As^{III} (van Lis et al., 2013). While As^{III} is also adsorbed onto Fe oxides and oxyhydroxides, its sorption strength with Fe surface complexation is weaker than As^V (Jonsson and Sherman, 2008). In environments where Fe is lacking and sulfur (S) is present, the solubility of As is potentially controlled by the precipitation of As in ASM (O'Day et al., 2004). The predominant species of S are sulfide (H₂S) and sulfate (SO₄²⁻), the most reduced and oxidized species, respectively. Microorganisms oxidize or reduce S depending on the redox conditions present in the aquifer (Tang et al., 2009). The microbial reduction of As^V and SO₄²⁻ can cause the biomineralization of As and ASM will be formed (Newman et al., 1997).

Recent evidence demonstrates the biological nature of the formation of ASM. Rittle et al. (1995) first proved the precipitation of As^{III} was due to biological SO₄²⁻ reduction. In 1997, Newman et al. (1997) discovered a new bacterial strain *Desulfotomaculum auripigmentum* sp. OREX-4 which was able to precipitate As₂S₃ through the heterotrophic reduction of As^V and SO₄²⁻. The biological precipitation of AsS by a thermophilic bacterium *Caloramator* strain YeAs (Ledbetter et al., 2007) and by a hyperthermophilic archaea *Pyrobaculum arsenaticum* sp. PZ6 (Huber et al., 2000); and, the formation of AsS nanotubes by *Shewanella* strains (Lee et al., 2007) have reinforced the evidence of ASM biogenesis. Furthermore, Demergasso et al. (2007) has demonstrated the biological origin of As₂S₃ in Andean sediments by analyzing the sulfur isotope ratios (³⁴S/³²S) in chemically and biologically formed ASM, and comparing it with the minerals found in the sediments. In addition, Saunders et al. (2008) evaluated the effect of SO₄²⁻ and electron donor addition on the As mobility in As contaminated groundwater, which resulted in a decrease of the dissolved As in the aquifer, attributed to the formation of FeAsS.

Several lab-scale experiments, conducted in microcosm or bioreactors, have been performed to study the biological precipitation of ASM at circumneutral or acidic pH. Most of these experiments studied the precipitation of ASM in Fe-containing systems (Kirk et al., 2010; Onstott et al., 2011). Fe-sulfide minerals, such as pyrite (FeS₂) or mackinawite (FeS) have lower solubility than the ASM, therefore they would precipitate first removing Fe and S from solution (Kirk et al., 2010; O'Day et al., 2004). In high SO₄²⁻ waters, Fe would become limited and the system would essentially behave as an Fe-poor environment, stressing the importance of understanding the formation of ASM in the absence of Fe.

The objective of this study was to determine the effect of the pH on the rate, extent and type of biological ASM formation in Fe-poor environments. In order to attain this objective, a series of batch experiments, with pH conditions ranging from 6.1 to 7.2, were performed using an anaerobic biofilm mixed culture as inocula with only trace levels of Fe. The batch experiments were amended with As^V and SO₄²⁻, and ethanol was used as electron donor. The main reactions occurring in the microcosms are summarized in Table 1. The precipitation of ASM was evaluated by measuring the total As and S concentration and speciation in solution. Likewise the solid phase was characterized by different spectroscopic techniques.

2. Materials and methods

2.1. Source of microorganisms

An anaerobic granular biofilm was obtained from full scale upflow anaerobic sludge bioreactor (UASB) from a beer brewery wastewater treatment plant Mahou (Guadalajara, Spain) (0.042 ± 0.002 g volatile suspended solids (VSS)/g wet wt). The sludge was examined for As content, and As level was below detectable limits (digestion of sludge using aqua regia and further analysis in the ICP-OES, see Section 2.6. Analytical methods).

2.2. Medium composition

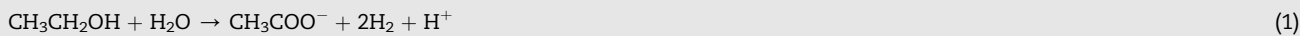
The basal medium was prepared using ultra pure water (Milli-Q system; Millipore) and contained (mg/L): K₂HPO₄ (600); NaH₂PO₄·2H₂O (899); NH₄Cl (280); MgCl₂·6H₂O (83); CaCl₂·2H₂O (10); yeast extract (20), and 1 mL/L of a trace element solution that was added to the medium to provide a final concentration of (μg/L): FeCl₃·4H₂O (2000); CoCl₂·6H₂O (2000); MnCl₂·4H₂O (500); AlCl₃·6H₂O (90); CuCl₂·2H₂O (30); ZnCl₂ (50); H₃BO₃ (50); (NH₄)₆Mo₇O₂₄·4H₂O (50); Na₂SeO₃·5H₂O (100); NiCl₂·6H₂O (50); EDTA (1000); resazurin (200); HCl 36% (1 μL). 0.75 mM of SO₄²⁻ was added as Na₂SO₄ and 0.5 mM of As^V Na₂HAsO₄·7H₂O. The electron donor used was ethanol to a final concentration of 14 mM by adding 283.3 μL/L. The experiments were flushed with N₂/CO₂ (80:20) to ensure anaerobic conditions. NaHCO₃ was used to control the pH of the solution from 6.1 (0.4 g/L NaHCO₃), 6.5 (1 g/L NaHCO₃), 6.85 (2 g/L NaHCO₃) and 7.2 (4 g/L NaHCO₃). 1.5 g VSS/L of sludge was added to the treatment, after being sieved and clean with Milli-Q water to remove any soluble contaminant.

2.3. Experimental incubations

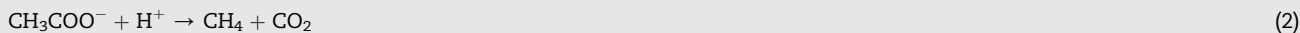
The biomineralization of ASM was evaluated in batch mode in 160 mL serum bottles containing 120 mL of the liquid medium. The liquid phase was flushed with N₂/CO₂ (80:20) for 10 min, then the 34 μL of ethanol were added to the proper treatments and quickly sealed with rubber septa and aluminum crimp seal. The headspace was flushed for 5 min needle in-needle out with N₂/CO₂ (80:20). The treatments were run in triplicate with one bottle dedicated to pH measurements and solid phase analysis. Proper controls were set up in parallel to

Table 1 – Summary of the important reaction to consider in the microcosm studies.

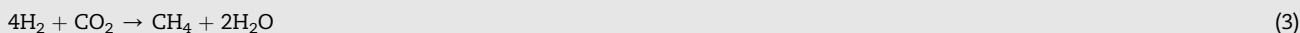
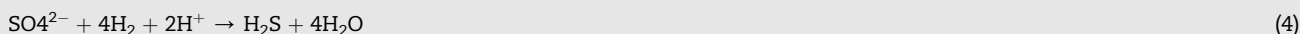
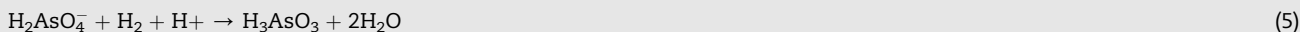
Ethanol acetogenesis:



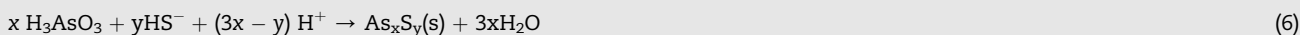
Acetoclastic methanogenesis:



Hydrogenotrophic methanogenesis:

Sulfate reduction coupled to H₂ oxidation:Arsenate reduction coupled to H₂ oxidation:

Mineralization:



x = y = 1, realgar (α-AsS) formation

x = 2; y = 3, orpiment (As₂S₃) formation

ensure the fidelity of the results. These controls were: (i) non-inoculated with As^V and ethanol, SO₄²⁻ and ethanol, or both, As^V and SO₄²⁻, and ethanol; (ii) inocula with just one of the electron acceptors and the ethanol; (iii) inocula with no electron acceptor; and, (iv) inocula with one electron acceptor but no ethanol. Non-inoculated controls were prepared under sterile conditions and the medium was autoclaved at 121 °C for 10 min. In the non-inoculated controls, ethanol was added after autoclaving to avoid degradation. The assays were incubated at 30 °C in the dark, and in an elliptical shaker (115 rpm).

2.4. Pourbaix diagrams

Pourbaix diagrams (E_n-pH diagrams) were used to understand the formation and stability of ASM for the experimental conditions (0.5 mM As^V, 0.25 mM SO₄²⁻). The thermodynamic data was obtained from Visual MinTEQA2 and National Bureau of Standards (NBS) databases and the diagrams were built using the W32-Stabcal modeling software.

2.5. As removal rate calculation

The As removal rate was obtained by calculating the slope for the percentage of As removal over time during the experiment, defined by the following equation:

$$\% \text{ As Removal Rate} = \left[\frac{\Delta(\% \text{ As Removal})}{\Delta(t)} \right]_0^t \quad (7)$$

The As removal rate was calculated for the period of increasing As removal until the steady state was reached.

2.6. Analytical methods

Liquid samples were taken from sealed serum flasks by piercing the stoppers using sterile syringes with 16-gauge needles. All samples were centrifuged (10 min, 14,000 g) after sampling and stored in polypropylene vials. As^V and SO₄²⁻ were analyzed by suppressed conductivity ion chromatography using a Dionex IC-3000 system (Sunnyvale, CA, USA) fitted with a Dionex IonPac AS11 analytical column

(4 × 250 mm) and AG16 guard column (4 mm × 40 mm). The injection eluent (KOH) was 30 mM for 10 min. Total As concentration was measured by using an inductively coupled plasma-optical emission spectrometry (ICP-OES) system model Optima 2100 DV from Perkin–Elmer TM (Shelton, CT, USA) monitored at wavelength 193.7 nm. H₂S was determined using the methylene blue method described by Truper (1964) and measured using an UV–visible spectrophotometer (Agilent 8453, Palo Alto, CA, USA). The measurement of H₂S provides the amount as H₂S in the liquid phase only. The total concentration of H₂S was calculated by considering the speciation of H₂S at the measured pH using the dissociation constants and the partition of H₂S between the liquid medium and the headspace at the incubation temperature.

Headspace samples in the batch experiments were taken with a pressure lock gas tight syringe (1710RN, 100 µl (22s/2"/2), Hamilton Company). Ethanol, acetate and CH₄ were monitored in an Agilent Technologies 7890A gas chromatography system with a Restek Stabilwax®-DA Column (30 m × 0.35 mm, ID 0.25 µm) with flame ionization detector, and He used as a carried gas.

Solid samples were taken under anaerobic conditions inside the anaerobic chamber (COY Laboratory Products Inc., Grass Lake, MI), to avoid any oxidation of the mineral. The solid samples were obtained by homogenizing and concentrating by centrifugation the solid phase contained in 50 mL to 1.5 mL. The solid phase was cleaned by centrifuging and replacing the supernatant with O₂ free Milli-Q water obtained by adding 100 mL of Milli-Q water to a 160 mL serum bottle,

and flushing it following the same procedure than for the experimental incubations. Solid phase was characterized using a Scanning Electron Microscopy (SEM) combined with energy dispersive spectroscopy (EDS), and K-edge X-ray absorption spectra (XAS) with X-ray absorption near-edge structure (XANES) and extended x-ray absorption fine-structure (EXAFS) according to the methodology previously described in the [Supplementary Information \(SI\)](#).

Measurements of pH, E_h and VSS were conducted according to standard methods (APHA, 1999).

3. Results

3.1. As and S biological transformations

The biological transformation of As and S and the precipitation of ASM was evaluated at three different pH conditions (6.1, 6.5 and 7.2) using ethanol as electron donor. Fig. 1 shows the evolution of As^V (A), total As (B), SO₄²⁻ (C) and total H₂S (soluble + volatile) (D), over the incubation time of the experiment at pH 6.1. Both As^V and SO₄²⁻ reduction were required for the formation of ASM to occur. When SO₄²⁻ was not amended in the treatment, As^V became reduced but the total As concentration in solution was not affected. Similarly, when As^V was not added to the treatment, SO₄²⁻ concentration decreased with a stoichiometric increment in H₂S concentration. But, when As^V and SO₄²⁻ were incubated together, the total As and S concentrations decreased, and 100% of the total

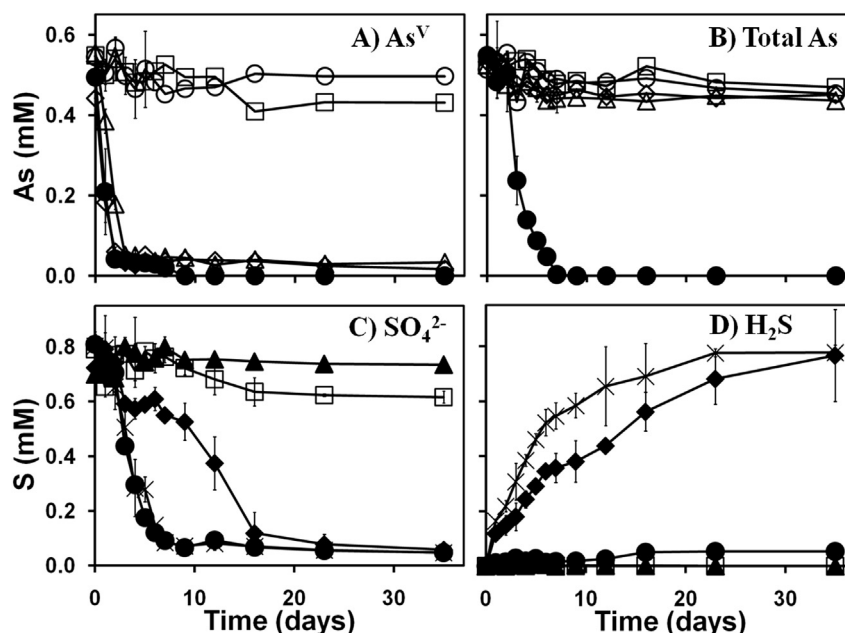


Fig. 1 – Precipitation of ASM through the biological mediated reduction of 0.5 mM of As^V and 0.75 mM of SO₄²⁻ using 14 mM of ethanol as the electron donor at pH 6.1. Dissolved As^V concentration of (A); total As concentration (B); SO₄²⁻ concentration (C); and total H₂S as the sum of H₂S(g) and all the aqueous species (mmol/L_{liq} or mM) (D). The complete treatment containing inoculum, As^V, SO₄²⁻ and ethanol (●); Inoculum, SO₄²⁻ and ethanol (×), Inoculum As^V and ethanol (◇), inoculum and SO₄²⁻ (◆), inoculum and As^V (Δ), inoculum and ethanol (+); Sterile controls with As^V and ethanol (○), the sterile control with SO₄²⁻ and ethanol (▲) and the combined reduction sterile control with SO₄²⁻ and As^V with ethanol (□). Treatments with value zero over the time course of the experiment are not shown: treatments lacking As in panels A and B, and treatments lacking S in panels C and D.

As was removed in only 9 d. Therefore, both the reduction of As^{V} and SO_4^{2-} must occur for the formation of ASM, as evidenced by the loss of total aqueous As and S.

The importance of the electron donor was evaluated in controls lacking ethanol. The addition of the electron donor was essential for ASM formation by promoting the reduction of SO_4^{2-} , which was limited in the controls lacking ethanol. Compared to the full treatment, the rate of SO_4^{2-} reduction in the absence of ethanol was 4.1-fold lower during the critical time period (days 1 and 9) when arsenic was being removed in the full treatment. In contrast, the rate of As^{V} reduction in the treatments without ethanol was as fast as in the ethanol-amended treatments. The addition of the electron donor greatly boosted the SO_4^{2-} reduction rate, enabling the formation of ASM.

The reduction of As^{V} and SO_4^{2-} in the non-inoculated controls was not noteworthy in comparison with the inoculated treatments. Total As and total S decreased by $10.7 \pm 2.6\%$ and $21.6 \pm 2.9\%$ respectively in non-inoculated treatments including both As^{V} and SO_4^{2-} . What little removal that did occur took place at the start and thereafter the concentrations were stable. The lack of important changes in the non-inoculated controls indicates that abiotic reactions are relatively unimportant compared with the biological reactions, stressing the significance of the biological transformations of As and S under the studied conditions.

The amount of total As and S removed in the treatments can be calculated by applying a mass balance in the system. The ratio of S loss to As loss ($S_{\text{loss}}/As_{\text{loss}}$) was used to predict mineral phase precipitation based on the expectation that an S/As of 1.5 and 1.0 corresponds to As_2S_3 and AsS , respectively. Fig. 2 compares the mass balances for S and As between different inoculated treatments after 35 d incubation at pH 6.1. In the absence of As^{V} , all the SO_4^{2-} reduced was recovered as H_2S , but if As^{V} was amended to the treatment, 0.71 mM of S as H_2S was missing from the experiment. Similarly, the total As concentration hardly decreased (15.3% of the total As) without SO_4^{2-} but the decrease was substantial (100% of the total As) if SO_4^{2-} was present in the treatment. The resulting $S_{\text{loss}}/As_{\text{loss}}$ ratio corresponded to 1.29 in the treatment amended with As^{V} and SO_4^{2-} . These results suggest the formation of a mixture of AsS and As_2S_3 .

The formation of ASM was confirmed by visual observation of a yellow precipitate just in the inoculated assays containing SO_4^{2-} and As^{V} . The formation of the mineral could be appreciated with the naked eye after 5 d of incubation. The amount of precipitate increased and the difference in the color of the medium between the complete inoculated treatment and the control missing As^{V} was very intense at day 12 (Fig. S1).

3.2. Role of pH on the precipitation of ASM and the removal of As

Two additional experiments were performed at pH 6.5 and 7.2. Similar as the results obtained for pH 6.1, As and S removal from solution was only significant in inoculated treatments containing both As^{V} and SO_4^{2-} . However, the extent and rate of As and S removal as well as the $S_{\text{loss}}/As_{\text{loss}}$ ratios varied depending on the pH. Table 2 provides the total As, SO_4^{2-} , H_2S , pH and $S_{\text{loss}}/As_{\text{loss}}$ ratio at five different times over the

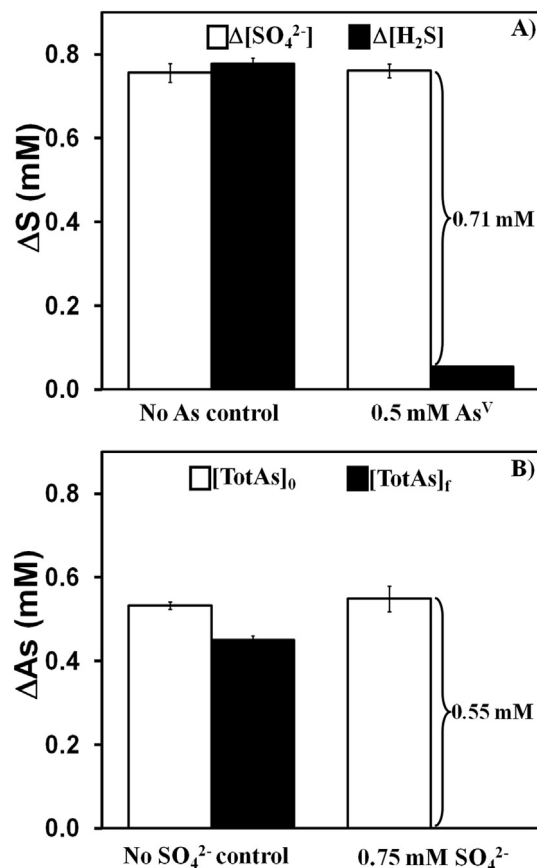


Fig. 2 – S and As concentration loss between day 0 and the end of the experiment (day 35) for the treatment at pH 6.1. Panel (A) show the S loss for the inoculated control with no As^{V} addition and for the complete treatment; the difference in SO_4^{2-} is represented in the open column and the formation of H_2S in the filled column. Panel (B) illustrates the total As loss in the inoculated control lacking SO_4^{2-} and in the complete treatment; initial total As concentration is represented with the open column and the final total As concentration with the filled column.

experiment for the three pH conditions, for the inoculated treatment with As^{V} and SO_4^{2-} amended with ethanol. The total loss of soluble As and S decreased as the pH conditions of the assay increased, which corresponded to more of the biogenic H_2S from SO_4^{2-} reduction being recovered in the medium (especially at pH 7.2). The ratio $S_{\text{loss}}/As_{\text{loss}}$ was 1.25–1.47 for the treatments at pH 6.1 and 6.5, but higher ratios were observed on days 9 and 12 at pH 7.2 (Table 2). These results suggest a pH dependence of the As removal and ASM formation.

The rate and extent of As removal was greatly impacted by the pH. Fig. 3 compares the percentage of As removal as a function of time for the three pH treatments. The percentage of As removed over the entire experiment was $93.9 \pm 0.6\%$ and $77.9 \pm 0.8\%$ at pH 6.5 and 7.2, respectively. The relationship between the extent and rate of As removal as a function of the pH is shown in Fig. 4. An inversely proportional dependency between the As removal and As removal rates was observed with pH. The percentage of As removed after 9 days was 2-fold

Table 2 – Experimental results at different times for the precipitation of As–S mineral treatments at different pH (6.1, 6.45 and 7.1).

Experiment	t_{exp} (d)	pH _t	[TotAs] _t (mM)	[SO ₄ ²⁻] _t (mM)	[H ₂ S] _t (mM)	S _{loss} /As _{loss} ^a
pH = 6.1	0	6.17	0.55 ± 0.01	0.81 ± 0.03	0.00 ± 0.00	–
	6	5.93	0.05 ± 0.02	0.12 ± 0.01	0.01 ± 0.00	1.34
	9	5.97	0.00 ± 0.00	0.07 ± 0.01	0.02 ± 0.01	1.32
	12	5.90	0.00 ± 0.00	0.09 ± 0.01	0.03 ± 0.01	1.25
	35	5.96	0.00 ± 0.00	0.05 ± 0.00	0.05 ± 0.00	1.29
pH = 6.45	0	6.44	0.51 ± 0.00	0.78 ± 0.02	0.00 ± 0.00	–
	6	6.49	0.25 ± 0.03	0.35 ± 0.02	0.05 ± 0.01	1.47
	9	6.49	0.10 ± 0.00	0.20 ± 0.02	0.04 ± 0.01	1.31
	12	6.47	0.07 ± 0.02	0.17 ± 0.04	0.04 ± 0.01	1.31
	34	6.49	0.03 ± 0.00	0.14 ± 0.01	0.03 ± 0.00	1.27
pH = 7.1	0	7.13	0.51 ± 0.01	1.09 ± 0.05	0.00 ± 0.00	–
	6	7.15	0.39 ± 0.01	0.87 ± 0.05	0.08 ± 0.01	1.27
	9	7.15	0.27 ± 0.03	0.57 ± 0.01	0.11 ± 0.00	1.80
	12	7.19	0.24 ± 0.00	0.38 ± 0.03	0.26 ± 0.02	1.72
	33	7.15	0.12 ± 0.00	0.38 ± 0.00	0.25 ± 0.04	1.19

$$S_{\text{loss}} = (\text{SO}_4^{2-} + \text{H}_2\text{S})_0 - (\text{SO}_4^{2-} + \text{H}_2\text{S})_t$$

$$\text{As}_{\text{loss}} = (\text{TotAs})_0 - (\text{TotAs})_t$$

^a S and As losses are defined as the difference between the total initial concentration and the concentration at time t.

higher at pH 6.1 than at pH 7.2. The rate of As removal was 3.4-fold higher at pH 6.1 than at pH 7.2 over the first 9 d of the experiment, and then it increased to 17-fold higher after H₂S started to accumulate at pH 7.2. The data fit with a linear equation over the pH range with a high correlation (*R*-squared values higher than 0.94). The results indicate a sharp pH-dependency in the near neutral range, with large rate enhancements at mildly acidic conditions.

An independent set of experiments was performed with an older sample of the anaerobic biofilm at different pHs. The same relationship was observed between As removal extent and rate as a function of the pH (results are shown in the [Supplementary Data](#)). The percentage of As removed was higher at the lower pH over a long term incubation. As removal and As removal rate were inversely proportionally dependent on the pH and the data also had a near perfect a linear equation, with a negative slope and a high correlation. The reproducibility of the results with a different sample of

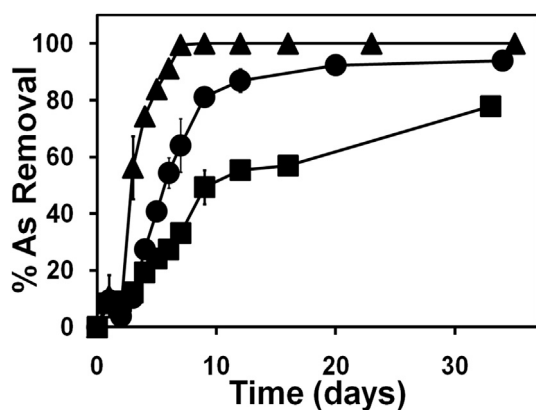


Fig. 3 – Total As removal over the course of the experiments shown as the As removal percentage at the three investigated pH 6.1 (▲), 6.5 (●) and 7.2 (■).

the anaerobic biofilm serves to validate the dependency of biogenic ASM formation on pH.

3.3. Mineral characterization

Solid samples from the three treatments were analyzed using SEM-EDS. Small particles of ASM were present as aggregates and on the surface of the bacteria. [Fig. 5](#) provides an SEM image and EDS analysis for two different points, on the surface of a bacterium (Point 1) and on a mineral aggregate (Point 2). The micrograph shows different bacteria surrounded by minerals. The EDS analysis demonstrates that the minerals are composed of As and S. These results confirm the close association between bacteria and mineral formation, supporting a microbial role in the formation of ASM. The solid mineral samples were further characterized using XAS.

XAS enabled the identification of As coordinative environment in precipitates formed at the two pH extremes of the conditions evaluated in the experiments (pH 6.1 and 7.2). [Fig. 6A](#) shows the XANES spectra for the two analyzed samples along with those of reference AsS and As₂S₃. The main XANES peak absorbance for As₂S₃ was shifted to slightly higher energy relative to that for AsS. However, this shift was within the resolution at the As edge and should not be used as a sole diagnostic for As coordinated in an As₂S₃ versus AsS structure. [Fig. 6B](#) shows the EXAFS spectrum of the two analyzed samples and the reference minerals. The solid formed at pH 6.1 had high similarity with AsS, but lacks the deep troughs of the AsS spectra at 7 to 8 and 9 to 10 k (Å⁻¹), suggesting the additional presence of As₂S₃ in the sample. The spectrum of the mineral formed at pH 7.2 is more similar to orpiment, but seemed to fall between the two mineral references. Linear combination fitting (LCF) of As K-edge EXAFS data suggests that the mineral formed at pH 6.1 was a mixture of AsS with As₂S₃, while the mineral formed at pH 7.2 corresponds more closely to As₂S₃, 63% AsS and 27% As₂S₃ and 38% AsS and 66% As₂S₃, respectively (sum ≠ 100% because the fits were not

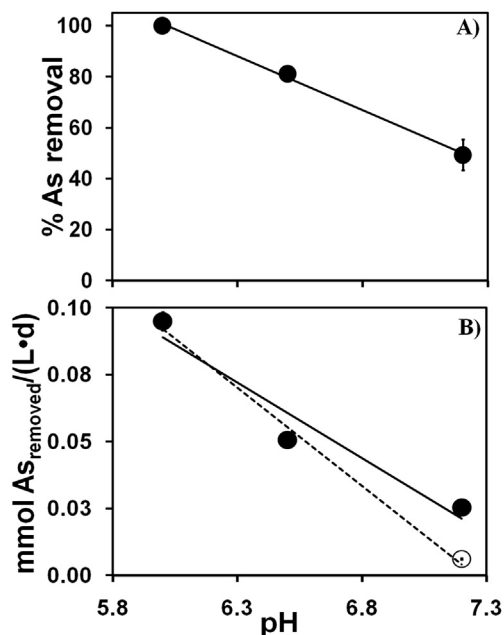


Fig. 4 – Relationship between the total As removal and the pH. Panel (A) illustrates the trend and linear regression line for As removal as a function of the pH at day 9. The linear regression equation was obtained and the relationship between the As removal and pH can be represented by the linear equation $\%As_{\text{removal}} = A - B \cdot \text{pH}$. The constants and the R-squared are: $A = 355.3\% \text{ As}$, $B = 42.4\% \text{ As}$, $R^2 = 0.9973$. Panel (B) shows the total As removal rate (mmol As/(L·d)) as a function of the pH. The total As removal rate was calculated using the slope for the first 6 d at pH 6.1, and for the first 9 d at pH 6.5. At pH 7.2, two different As removal rates were observed, high rate, from day 0–9 (●), and a lower rate, from day 9 until the end of the experiment (○). The rate of As removal is related to the pH by linear regression equations considering the higher rate at pH 7.2 (continuous line) and the lower rate at pH 7.2 (dashed line). The constants and the R-squared are: higher rate at pH 7.2, $A = 0.4286 \text{ mmol As/(L·d)}$, $B = 0.0566 \text{ mmol As/(L·d)}$, and $R^2 = 0.9374$; lower rate at pH 7.2, $A = 0.5324 \text{ mmol As/(L·d)}$, $B = 0.0734 \text{ mmol As/(L·d)}$, and $R^2 = 0.9911$.

normalized). The XANES fits indicated that the speciation of the pH 6.1 sample was 65% AsS and 33% As₂S₃ and the speciation of the pH 7.2 sample was 32% AsS and 67% As₂S₃. The occurrence of AsS and As₂S₃ was fully confirmed by the XAS characterization.

3.4. Ethanol as the electron donor source and the production of acetate and CH₄

In order to monitor the electron-donating process, the conversion of ethanol to acetate and CH₄ was measured. The degradation pathway of ethanol to CH₄ by the microbial consortium in the anaerobic biofilm can be evaluated by studying the treatment lacking As^V and SO₄²⁻ addition. Ethanol is transformed to acetate and hydrogen (H₂) by acetogenic

bacteria (Eq. (1)). Both acetate and H₂ are used by methanogens (Eqs. (2) and (3)) to produce CH₄. As can be appreciated in Fig. 7, in the treatment missing SO₄²⁻ and As^V, ethanol concentration decreased quickly after just one day of incubation, accompanied by a small initial accumulation of acetate and subsequently the formation of CH₄. CH₄ production increased rapidly until reaching a concentration of $8.7 \pm 0.4 \text{ mmol/L}_{\text{liq}}$. Thereafter, CH₄ kept increasing for the rest of the experiment at a lower rate. By the end of the experiment, the production of CH₄ was $13.9 \pm 0.7 \text{ mmol/L}_{\text{liq}}$. These results illustrate the rapid transformation of ethanol to acetate and subsequently to CH₄. The addition of As^V and SO₄²⁻ to the treatments can potentially impact the utilization of ethanol since electron equivalents (e⁻ eq) could be used for their reduction. The H₂S and As^{III} formed from the reduction could potentially inhibit the activity of the methanogens.

Ethanol utilization rate was the same in the presence or absence of SO₄²⁻, indicating that the addition of SO₄²⁻ and its reduction to H₂S did not affect the metabolic activity of acetogens. In addition, the pattern of acetate accumulation and subsequent consumption as well as the profile of CH₄ production was similar in both cases. The CH₄ production was however slightly lower in the presence of SO₄²⁻. The difference between the CH₄ produced was 1.1 mmol/L_{liq}, since 3.2 mmol/L_{liq} of H₂ would be required to reduce the supplied 0.8 mM of SO₄²⁻ to H₂S, 0.8 mmol/L_{liq} less CH₄ would have been expected in the treatment with SO₄²⁻. This analysis supports the expectation that H₂ from ethanol conversion was utilized as the electron donor for SO₄²⁻ reduction.

The inhibitory impact of As^V to the acetogenic and methanogenic activity was also evaluated. The presence of As greatly reduced the rate of ethanol conversion, and it inhibited the methanogenic activity. Ethanol concentration decreased at a much lower rate in the presence compared to the absence of As. In the presence of As, the acetate concentration increased until day 5, when it reached $5.1 \pm 0.9 \text{ mM}$; thereafter, the concentration was stable until the end of the experiment. The accumulated acetate was clearly not being used as a substrate by the methanogens to produce CH₄. CH₄ formed slowly throughout the course of the experiment, and the production rate was approximately 10-fold less than in the treatment with no As. These results demonstrate that the presence of As can delay the utilization of ethanol by acetogenic bacteria, and it greatly inhibit the acetoclastic methanogenic activity.

In treatments receiving both SO₄²⁻ and As^V, the formation of ASM reversed the methanogenic inhibition by As. The inhibition reversal did not occur immediately but instead corresponded to the moment in time when full precipitation of ASM minerals occurred on day 8 (Fig. 7). Consequently during the first 8 days, the full treatment (receiving both As^V and SO₄²⁻) behaved the same as the treatment with just As^V addition. There was a delay in the ethanol utilization, with an initial accumulation of acetate and no CH₄ production in both cases (Fig. 7). On day 9, after the entire total soluble As was removed (Fig. 1) due to ASM precipitation, the inhibition reversed. The accumulated acetate decreased to low levels and the CH₄ production all of sudden commenced, reaching a final production of $8.9 \pm 0.9 \text{ mmol/L}_{\text{liq}}$ (Fig. 7). Therefore, the removal of As by the biogenic formation of ASM rendered the

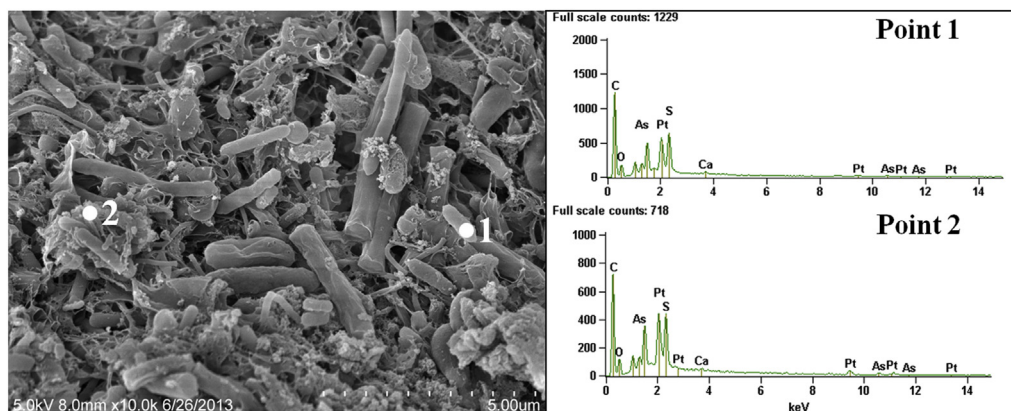


Fig. 5 – SEM-EDS analysis of the precipitate from the complete treatment at pH 6.1 containing 0.5 mM As^V, 0.75 mM SO₄²⁻ and 14 mM ethanol after 21 days of incubation.

As non-bioavailable and thus the As was no longer capable of causing microbial toxicity.

4. Discussion

The results taken as a whole demonstrate that the biological reduction of As^V and SO₄²⁻ by an anaerobic mixed culture biofilm leads to the formation of ASM in Fe-poor environments, leading to the immobilization of As to non-bioavailable forms. The biomineralization of the ASM depended strongly on the pH conditions in the near neutral range. The amount and rate of As removal were highly enhanced at mildly acidic conditions. Ethanol was readily used as an electron donor source to stimulate the reduction of As^V and SO₄²⁻. The presence of soluble As was found to completely inhibit the activity

of the methanogens in the biofilm inoculum; however, the insolubilization of As by biogenic ASM formation reversed the inhibition.

4.1. Microbial reduction of As^V and SO₄²⁻ promotes the bioprecipitation of ASM

The biogenic formation of ASM can be attained by the combined reduction of As^V and SO₄²⁻. A mixed culture biofilm from a methanogenic environment, which was not previously exposed to high As levels, readily reduced As^V. As^V and SO₄²⁻ can be biologically reduced by a pure or by a mixed culture. Several SO₄²⁻-reducing bacteria have been reported as As^V-reducing bacteria (Macy et al., 2000). But only five strains of three bacterial genera, *Desulfotomaculum* (Newman et al., 1997), *Caloramator* (Ledbetter et al., 2007) and *Shewanella* (Lee

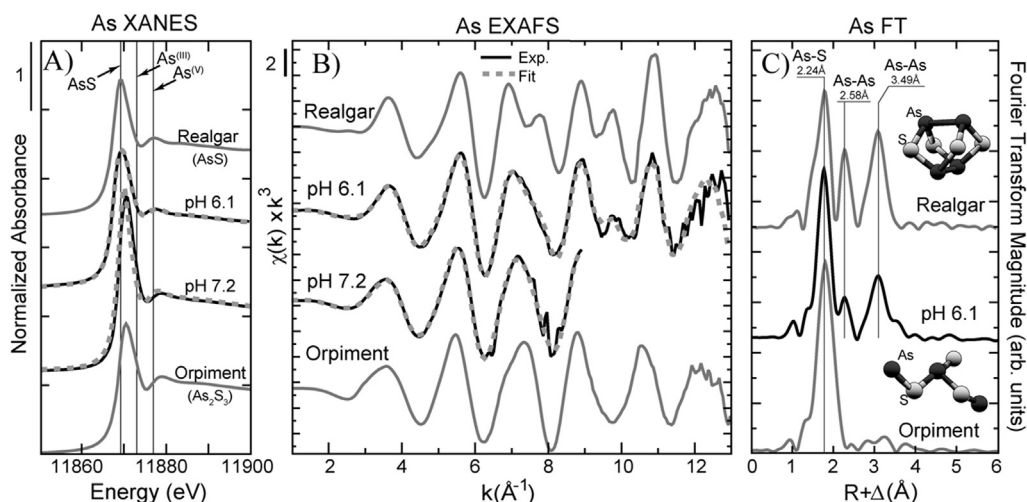


Fig. 6 – Arsenic K- α x-ray absorption spectra of the solids precipitated in the experiments at pH 6.1 and 7.2. Panel A shows the XANES spectra (solid lines) for As–S mineral fit (stippled lines) by least squares linear combination to standards (gray lines) of realgar (AsS) and orpiment (As₂S₃), vertical lines indicate the diagnostic As species position (± 1 eV): 11869 = arsenic sulfide; 11872 = As^{III}; 11875 = As^V. Panel B shows the EXAFS spectra for the experimental data (black lines) and least squares linear combination fits (stippled lines) to As–S minerals. Fits and reported error are given in Table S1. The Fourier Transform (FT) of the references and the pH 6.1 sample are shown in Panel C; vertical bars indicate As-backscatter distances. The FT is not shown for pH 7.2 because EXAFS were cut at k (\AA^{-1}) = 9 and did not allow comparison to pH = 6.1.

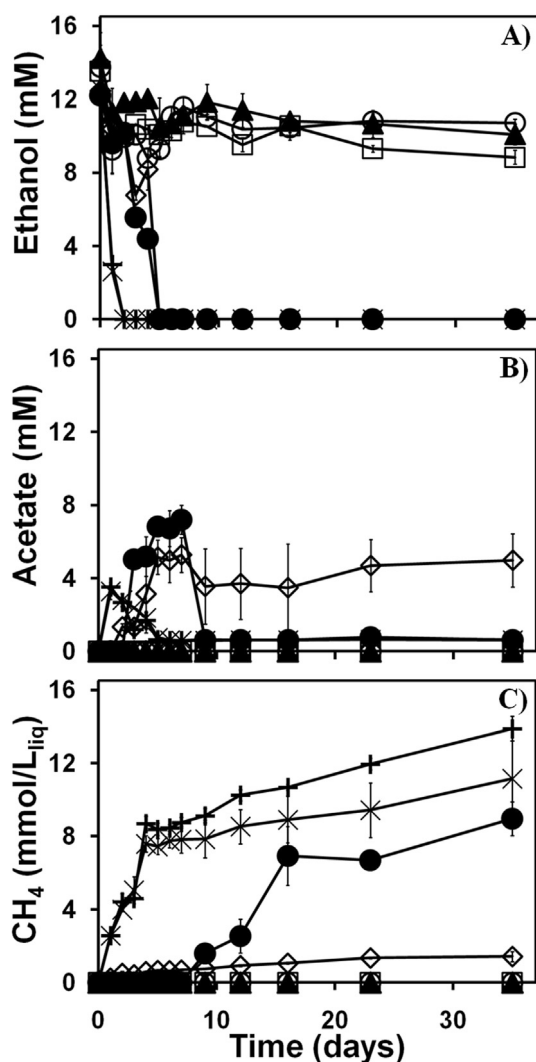


Fig. 7 – Conversion of 14 mM ethanol in the experiment conducted at pH 6.1. Panels show the ethanol concentration (A); acetate concentration (B); and, CH_4 production (C). The complete treatment containing inoculum, As^{V} , SO_4^{2-} and ethanol (\bullet); Inoculum, SO_4^{2-} and ethanol (\times), Inoculum As^{V} and ethanol (\diamond), inoculum and SO_4^{2-} (\blacklozenge), inoculum and As^{V} (Δ), inoculum and ethanol ($+$); Sterile controls with As^{V} and ethanol (\circ), the sterile control with SO_4^{2-} and ethanol (\blacktriangle) and the sterile control with SO_4^{2-} , As^{V} and ethanol (\square). Treatments lacking ethanol addition (with zero values over the time course of the experiment) are not shown.

et al., 2007) have been reported to precipitate As_2S_3 , AsS and As-S nanotubes, respectively; and, a hyperthermophilic archaea genus, *Pyrobaculum* (Huber et al., 2000) can precipitate AsS . However, the presence of As^{V} and SO_4^{2-} -reducers in a mixed culture has been proven to promote the precipitation of ASM in natural environments (Demergasso et al., 2007; Saunders et al., 2008) as well as in a laboratory scale bioreactor (Battaglia-Brunet et al., 2012). In this study, the anaerobic mixed culture biofilm reduced As^{V} and SO_4^{2-} when both were amended into the same treatment, causing biogenesis of

ASM which effectively immobilized the soluble As . The natural co-occurrence between As^{V} and SO_4^{2-} -reducing bacteria can explain the ability of anaerobic microorganisms to promote the bioprecipitation of ASM.

The addition of ethanol as exogenous electron donor was not a requirement to achieve As^{V} reduction. In the treatments lacking ethanol, there are two sources of e^- eq to support the reduction of As^{V} , the endogenous decay of the mixed culture biofilm and the degradation of the yeast extract amended to support the growth of the biofilm. The potential of methanogenic sludge to reduce As^{V} without the addition of an electron donor has been reported before (Sierra-Alvarez et al., 2005). Furthermore, the contribution of the endogenous substrate decay in a comparable methanogenic biofilm corresponded to 16–21 e^- meq/g VSS, available due to the hydrolysis of biomass in the sludge over 30 d (Tapia-Rodriguez et al., 2010). The initial rate of endogenous decay was found to be 0.4 to 1.1 e^- meq/g VSS.d. According to these results, the biofilm can donate 24–31 e^- meq/L electron donor at a rate of 0.6–1.7 e^- meq/(L.d) with the 1.5 gVSS/L used in the experiments. In addition to the e^- eq donated by the endogenous substrate decay, the degradation of the yeast extract (20 mg/L) could provide up to 3.1 e^- meq/L. Therefore, the amount of e^- eq released by the decay of the biofilm and the yeast extract would be more than ample to support the reduction of 0.5 mM of As^{V} (1 e^- meq/L).

The addition of an exogenous electron donor greatly enhanced SO_4^{2-} reduction. This coincided with a previous study where ethanol was found to be an effective electron donor promoting enhanced SO_4^{2-} reduction in an anaerobic granular sludge biofilm beyond the endogenous rate (Liu et al., 2010). The reduction of 0.8 mM of SO_4^{2-} to H_2S requires 6.4 e^- meq/L, which are available from the endogenous substrate decay and the degradation of yeast extract; however, an initial competition between SO_4^{2-} -reducing bacteria and methanogens delayed the reduction of SO_4^{2-} . The competition for e^- eq between SO_4^{2-} -reducing bacteria and methanogens has been reported in several studies in the past. SO_4^{2-} reducers will outcompete methanogens for the electron donor utilization, since they have a higher substrate affinity for H_2 , but an initial competition would occur due to lower initial numbers of SO_4^{2-} reducers than methanogens in a methanogenic sludge (Elferink et al., 1994).

4.2. Slightly increasing the pH decreased the amount of As removal and percentage of AsS in the mineral

Small variations in the pH affected the removal of As from the system. The extent and rate of As and S removal from aqueous solution were highest at the lower pH conditions corresponding to mildly acidic pH values. When the pH increased, less H_2S was removed due to ASM formation. High H_2S concentrations at neutral pH are known to favor the formation of thioarsenite species (Wilkin et al., 2003), limiting the elimination of soluble As by biomineralization. Newman et al. (1997) studied the chemical precipitation of As_2S_3 at different pH values and different H_2S concentrations. As_2S_3 was readily precipitated at pH lower than 7 but not at higher pH values when the H_2S concentration was 0.1 mM. Increasing the H_2S concentration to 1 mM caused the minimum pH required for As_2S_3 precipitation to decrease to 6.6.

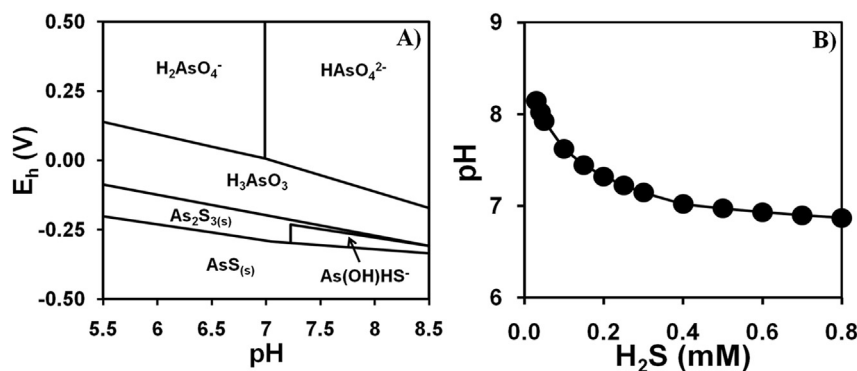


Fig. 8 – Predicted stable mineral and aqueous phases at equilibrium, including thioarsenite species. Panel A: Pourbaix diagram for As minerals at 25 °C and 1 atm showing the stability fields for solid phases at the conditions the orpiment and realgar, in a solution with 0.5 mM of As and 0.25 mM of S. Panel B: Minimum pH enabling formation of thioarsenite species as a function of the H₂S equilibrium concentration, ranging from 0 to 0.75 mM (maximum H₂S production due to SO₄²⁻ reduction).

ASM formation is impacted by the stoichiometry of the available As^{III} and H₂S, which will be dictated by the reduction of As^V and SO₄²⁻. Microorganisms gain more energy from the dissimilatory reduction of As^V compared to SO₄²⁻ reduction, thus As^V reduction is expected to proceed first. A bioenergetic analysis of the redox pair shows that As^V/As^{III} has higher standard reduction potential (60 mV) than SO₄²⁻/H₂S (–220 mV) (Hoefst et al., 2004). In this study, As^V was reduced first prior to SO₄²⁻ reduction, but it is not clear if it was due to an energetic advantage or the fact that there was a 2 d lag phase before SO₄²⁻ reduction started, both in the presence and in the absence of As^V. Hence, As^{III} was already formed before H₂S started to accumulate, favoring the biomineralization of As^{III}–H₂S and removing H₂S from the medium. This conclusion is in agreement with the observations made by Newman et al. (1997). *D. auropigmentum* first reduced As^V and then SO₄²⁻, allowing the precipitation of As₂S₃, while another tested bacterium, *Desulfobulbus propionicus*, that quickly reduced SO₄²⁻ before reducing As^V, was not able to promote the formation of ASM. The concomitant reduction of As^V and thio-sulfate (S₂O₃²⁻) by *Shewanella* strain HN-41 also promoted the precipitation of As–S nanotubes (Lee et al., 2007). Therefore, biological activity can enhance the precipitation of ASM by controlling the rate of As^{III} and H₂S formation in a favorable stoichiometric ratio.

The pH changes also affected the mineralogy of the precipitate. The S_{10ss}/As_{10ss} ratio and XAS analysis showed an increase in As₂S₃ proportion over AsS at the higher pH values. The stoichiometric calculations from the S_{10ss}/As_{10ss} ratios indicates 70% AsS and 30% As₂S₃ at pH 6.1 which are in good agreement with XAS characterization results of the solid phase. However, the ratios during days 9 and 12 at pH 7.2 indicate 100% As₂S₃ which differs from the solid characterization results, 67% and 66% orpiment by XANES and EXAFS respectively. A plausible explanation is that both the stoichiometric ratio and the spectral data obtained for pH 7.2 have a higher associated error compared to data obtained at pH 6.1. Nevertheless, both the solid characterization and the stoichiometric ratio analysis correctly predict an increase in As₂S₃ percentage with increasing pH. The relationship between the

mineral phase proportion and the pH has not been studied before. The difference in behavior with pH can be explained by thermodynamic relationships.

The prediction of ASM species in a solution was evaluated by creating Pourbaix diagrams. Fig. 8A shows the Pourbaix diagram for an As concentration of 0.5 mM and S concentration of 0.25 mM (the maximum concentration of H₂S at equilibrium in the pH 7.2 experiment). At the studied pH and E_h range (E_h = –200 ± 50 mV, measured), As₂S₃ and AsS are the minerals expected to precipitate for pH values close to 6 within the range of E_h in the treatments. With increasing pH, the formation of AsS is limited to more reducing conditions, and As₂S₃ is the more likely precipitate up to a pH of 7.0, thereafter, thioarsenites species become predominant, limiting the precipitation of ASM. The thermodynamic stability areas for As₂S₃ and AsS predicted in this study are similar to the Pourbaix diagrams constructed by Lu and Zhu (2011) for a system containing 1 mM of S and As. Fig. 8B was built to show the formation of thioarsenites as a function of the pH and H₂S concentration. As the concentration of H₂S increases, the minimum pH at which thioarsenites could be formed decreases. The same trend was predicted by Wilkin et al. (2003) when studying the solubility of As in the presence of S. In conclusion, for the experimental E_h range, the formation of As₂S₃ and AsS is expected over the mildly acidic range of pH; at circumneutral and higher pH values, the formation of thioarsenite species becomes dominant and limits the precipitation of ASM, however, for any precipitation that does occur it would be predominantly in the form of As₂S₃.

4.3. As toxicity effect on the methanogenic activity

Soluble As was highly toxic to the methanogenic archaea community. The soluble As^{III} formed from the reduction of As^V caused a severe inhibition in the methanogenic activity, as demonstrated by the accumulation of acetate and the extremely low CH₄ production. However, the inhibition was largely attenuated by the removal of As throughout the precipitation of ASM. The high toxicity of As^{III} in methanogenic consortium has been established by Sierra-Alvarez et al.

(2004). Very low As^{III} concentrations are enough to greatly inhibit the methanogenic activity, the 80% inhibitory concentrations were 23.5 μM and 79.2 μM, for the acetoclastic and hydrogenotrophic methanogenesis, respectively. The As^{III} concentration in this study was 500 μM. The high concentration of As^{III} (produced by the bioreduction of As^V) greatly inhibited the metabolic activity of the methanogenic community.

4.4. Conclusions

- This study demonstrates that the biological reduction of As^V and SO₄²⁻ by a mixed microbial culture in a methanogenic biofilm can be harnessed to precipitate ASM.
- The extent and rate of As removal is highly influenced by the pH, with the highest rates achieved at mildly acidic conditions.
- The pH would also impact the mineralogical composition of the ASM, with an increase in orpiment compared to realgar at neutral pH.
- Arsenic biomineralization can potentially be used to promote the immobilization of As groundwaters by stimulating the As^V and SO₄²⁻ reducing bacteria.

Acknowledgments

The work presented here was funded by a grant of the National Institute of Environment and Health Sciences-supported Superfund Research Program (NIH ES-04940). Portions of this research were carried out at Stanford Synchrotron Radiation Laboratory, a National User Facility operated by Stanford University on behalf of the U.S. Department of Energy, Office of Basic Energy Sciences. We are also grateful to the University Spectroscopy and Imaging Facility at the University of Arizona for the SEM-EDS analysis. This work was partially funded by a Water Sustainability Program Fellowship, The University of Arizona, awarded to Lucia Rodriguez-Freire.

Appendix A. Supplementary data

Supplementary data related to this article can be found at <http://dx.doi.org/10.1016/j.watres.2014.08.016>.

REFERENCES

APHA, 1999. Standard Methods for the Examination of Water and Wastewater. APHA, AWWA and WEF, Washington D.C.

Battaglia-Brunet, F., Crouzet, C., Burnol, A., Coulon, S., Morin, D., Joulain, C., 2012. Precipitation of arsenic sulphide from acidic water in a fixed-film bioreactor. *Water Res.* 46 (12), 3923–3933.

Demergasso, C.S., Chong, G., Escudero, L., Mur, J.J.P., Pedros-Alio, C., 2007. Microbial precipitation of arsenic sulfides in Andean salt flats. *Geomicrobiol. J.* 24 (2), 111–123.

Elferink, S.J.W.H., Visser, A., Pol, L.W.H., Stams, A.J.M., 1994. Sulfate reduction in methanogenic bioreactors. *FEMS Microbiol. Rev.* 15 (2–3), 119–136.

Hoefel, S.E., Kulp, T.R., Stolz, J.F., Hollibaugh, J.T., Oremland, R.S., 2004. Dissimilatory arsenate reduction with sulfide as electron donor: experiments with Mono Lake Water and isolation of strain MLMS-1, a chemoautotrophic arsenate respirer. *Appl. Environ. Microbiol.* 70 (5), 2741–2747.

Huber, R., Sacher, M., Vollmann, A., Huber, H., Rose, D., 2000. Respiration of arsenate and selenate by hyperthermophilic archaea. *Syst. Appl. Microbiol.* 23 (3), 305–314.

Jonsson, J., Sherman, D.M., 2008. Sorption of As(III) and As(V) to siderite, green rust (fougerite) and magnetite: implications for arsenic release in anoxic groundwaters. *Chem. Geol.* 255 (1–2), 173–181.

Kirk, M.F., Roden, E.E., Crossey, L.J., Brearley, A.J., Spilde, M.N., 2010. Experimental analysis of arsenic precipitation during microbial sulfate and iron reduction in model aquifer sediment reactors. *Geochim. et Cosmochim. Acta* 74 (9), 2538–2555.

Ledbetter, R.N., Connon, S.A., Neal, A.L., Dohnalkova, A., Magnuson, T.S., 2007. Biogenic mineral production by a novel arsenic-metabolizing thermophilic bacterium from the Alvord Basin, Oregon. *Appl. Environ. Microbiol.* 73 (18), 5928–5936.

Lee, J.H., Kim, M.G., Yoo, B.Y., Myung, N.V., Maeng, J.S., Lee, T., Dohnalkova, A.C., Fredrickson, J.K., Sadowsky, M.J., Hur, H.G., 2007. Biogenic formation of photoactive arsenic-sulfide nanotubes by *Shewanella* sp. strain HN-41. *Proc. Natl. Acad. Sci. USA* 104 (51), 20410–20415.

Liu, B., Wu, W.F., Zhao, Y.J., Gu, X.Y., Li, S., Zhang, X.X., Wang, Q., Li, R.H., Yang, S.G., 2010. Effects of ethanol/SO₄²⁻ ratio and pH on mesophilic sulfate reduction in UASB reactors. *Afr. J. Microbiol. Res.* 4 (21), 2215–2222.

Lu, P., Zhu, C., 2011. Arsenic Eh-pH diagrams at 25 degrees C and 1 bar. *Environ. Earth Sci.* 62 (8), 1673–1683.

Macy, J.M., Santini, J.M., Pauling, B.V., O'Neill, A.H., Sly, L.I., 2000. Two new arsenate/sulfate-reducing bacteria: mechanisms of arsenate reduction. *Arch. Microbiol.* 173 (1), 49–57.

Murcott, S., 2012. Arsenic Contamination in the World. An International Sourcebook 2012. IWA Publishing, London.

Newman, D.K., Beveridge, T.J., Morel, F.M.M., 1997. Precipitation of arsenic trisulfide by *Desulfotomaculum auripigmentum*. *Appl. Environ. Microbiol.* 63 (5), 2022–2028.

O'Day, P.A., Vlassopoulos, D., Root, R., Rivera, N., 2004. The influence of sulfur and iron on dissolved arsenic concentrations in the shallow subsurface under changing redox conditions. *Proc. Natl. Acad. Sci. USA* 101 (38), 13703–13708.

Onstott, T.C., Chan, E., Polizzotto, M.L., Lanzon, J., DeFlaun, M.F., 2011. Precipitation of arsenic under sulfate reducing conditions and subsequent leaching under aerobic conditions. *Appl. Geochem.* 26 (3), 269–285.

Rittle, K.A., Drever, J.I., Colberg, P.J.S., 1995. Precipitation of arsenic during bacterial sulfate reduction. *Geomicrobiol. J.* 13 (1), 1–11.

Saunders, J.A., Lee, M.K., Shamsudduha, M., Dhakal, P., Uddin, A., Chowdury, M.T., Ahmed, K.M., 2008. Geochemistry and mineralogy of arsenic in (natural) anaerobic groundwaters. *Appl. Geochem.* 23 (11), 3205–3214.

Sierra-Alvarez, R., Cortinas, I., Yenal, U., Field, J.A., 2004. Methanogenic inhibition by arsenic compounds. *Appl. Environ. Microbiol.* 70 (9), 5688–5691.

Sierra-Alvarez, R., Field, J.A., Cortinas, I., Feijoo, G., Teresa Moreira, M., Kopplin, M., Jay Gandolfi, A., 2005. Anaerobic microbial mobilization and biotransformation of arsenate adsorbed onto activated alumina. *Water Res.* 39 (1), 199–209.

Tang, K., Baskaran, V., Nemat, M., 2009. Bacteria of the sulphur cycle: an overview of microbiology, biokinetics and their role in petroleum and mining industries. *Biochem. Eng. J.* 44 (1), 73–94.

Tapia-Rodriguez, A., Luna-Velasco, A., Field, J.A., Sierra-Alvarez, R., 2010. Anaerobic bioremediation of hexavalent

- uranium in groundwater by reductive precipitation with methanogenic granular sludge. *Water Res.* 44 (7), 2153–2162.
- Truper, H.G., 1964. Sulphur metabolism in *Thiorhodaceae* II. stoichiometric relationship of CO₂ fixation to oxidation of hydrogen sulphide and intracellular sulphur in *Chromatium okenii*. *Ant. Van Leeuwenhoek J. Microbiol. Serology* 30 (4), 385.
- US-EPA, 2001. National Primary Drinking Water Regulations; Arsenic and Clarifications to Compliance and New Source Contaminants Monitoring.
- van Lis, R., Nitschke, W., Duval, S., Schoepp-Cothenet, B., 2013. Arsenics as bioenergetic substrates. *Biochim. et Biophys. Acta-Bioenerg.* 1827 (2), 176–188.
- Welch, A.H., Westjohn, D.B., Helsel, D.R., Wanty, R.B., 2000. Arsenic in ground water of the United States: occurrence and geochemistry. *Ground Water* 38 (4), 589–604.
- Wilkin, R.T., Wallschläger, D., Ford, R.G., 2003. Speciation of arsenic in sulfidic waters. *Geochem. Trans.* 4, 1–7.